Virology 462-463 (2014) 34–41

Contents lists available at ScienceDirect

Virology

journal homepage: www.elsevier.com/locate/yviro

Brief Communication

The lysine methyltransferase SMYD3 interacts with hepatitis C virus NS5A and is a negative regulator of viral particle production

Carol-Ann Eberle [a], Margarita Zayas [b], Alexey Stukalov [a], Andreas Pichlmair [a,c], Gualtiero Alvisi [b,d], André C. Müller [a], Keiryn L. Bennett [a], Ralf Bartenschlager [b,*], Giulio Superti-Furga [a,**]

[a] CeMM Research Center for Molecular Medicine of the Austrian Academy of Sciences, Lazarettgasse 14, AKH BT 25.3, 1090 Vienna, Austria
[b] Department of Infectious Diseases, Molecular Virology, Heidelberg University, Im Neuenheimer Feld 345, 69120 Heidelberg, Germany
[c] Max-Planck Institute of Biochemistry, Am Klopferspitz 18, 82152 Martinsried, Germany
[d] Department of Molecular Medicine, Via Gabelli 63, 35121 Padua, Italy

ARTICLE INFO

Article history:
Received 4 February 2014
Returned to author for revisions
28 February 2014
Accepted 14 May 2014
Available online 14 June 2014

Keywords:
SMYD3
NS5A
HCV
TAP-MS
Virus particle assembly

ABSTRACT

Hepatitis C virus (HCV) is a considerable global health and economic burden. The HCV nonstructural protein (NS) 5A is essential for the viral life cycle. The ability of NS5A to interact with different host and viral proteins allow it to manipulate cellular pathways and regulate viral processes, including RNA replication and virus particle assembly. As part of a proteomic screen, we identified several NS5A-binding proteins, including the lysine methyltransferase SET and MYND domain containing protein 3 (SMYD3). We confirmed the interaction in the context of viral replication by co-immunoprecipitation and co-localization studies. Mutational analyses revealed that the MYND-domain of SMYD3 and domain III of NS5A are required for the interaction. Overexpression of SMYD3 resulted in decreased intracellular and extracellular virus titers, whilst viral RNA replication remained unchanged, suggesting that SMYD3 negatively affects HCV particle production in a NS5A-dependent manner.

Introduction

Hepatitis C virus (HCV) is a positive-sense, single-stranded RNA virus and among the leading causes of chronic hepatitis, a condition often complicated by liver cirrhosis, steatosis and cancer. With an estimated ~170 million people persistently infected worldwide, HCV constitutes a major global health and economic burden (Davis et al., 2011; Mohd Hanafiah et al., 2013). The viral genome consists of a single-strand RNA molecule of ~9.6-kb, encoding only a single polyprotein, which is processed into the three structural proteins core, E1, E2, and the seven non-structural (NS) proteins, p7, NS2, NS3, NS4A, NS4B, NS5A and NS5B (reviewed in (Bartenschlager et al., 2011)). NS5A is a multifunctional, RNA-binding phosphoprotein with key functions in HCV replication and assembly. In addition, NS5A manipulates various cellular pathways to generate an intracellular environment favoring viral replication (Cordek et al., 2011).

The protein is composed of three domains (DI, DII and DIII) that are connected by trypsin-sensitive low complexity sequences (LCSI and II) and contains an N-terminal amphipatic α-helix which tethers NS5A to intracellular membranes (Brass et al., 2002; Penin et al., 2004; Reiss et al., 2011; Tellinghuisen et al., 2004). DI and DII are required for genome replication, whereas DIII is essential for the generation of infectious virus particles (Appel et al., 2008; Masaki et al., 2008; Tellinghuisen et al., 2008b). Thus far, no enzymatic activity has been ascribed to NS5A and although it has been subject to intensive research, the molecular events required for the various effects of NS5A are far from being fully understood. Nevertheless, differential interactions with host as well as viral proteins seem to form the basis of NS5A function (Cordek et al., 2011).

As part of a large-scale proteomic survey of virus–host protein interactions, we identified several cellular binding partners of NS5A (genotype 1b) using a tandem-affinity purification (TAP) mass spectrometry (MS) approach (Pichlmair et al., 2012). Included among the highest ranking proteins was the SET and MYND domain containing protein 3 (SMYD3). SMYD3 is a lysine methyltransferase (KMT) which catalyzes di- and trimethylation of histones H3 and H4, implicating it in transcriptional regulation (Cock-Rada et al., 2012; Foreman et al., 2011; Hamamoto et al.,

* Corresponding author. Tel.: +49 (0)6221 56 4569.
** Corresponding author. Tel.: +43 1 40160 70 001.
E-mail addresses: Ralf.Bartenschlager@med.uni-heidelberg.de (R. Bartenschlager), gsuperti@cemm.oeaw.ac.at (G. Superti-Furga).

http://dx.doi.org/10.1016/j.virol.2014.05.016

2004). In addition, SMYD3 has also been shown to methylate the vascular endothelial growth factor receptor 1 (VEGFR1) and enhance its kinase activity (Kunizaki et al., 2007). However, there are no reports regarding a role of SMYD3 in the HCV life cycle.

Results and discussion

To follow up and expand on the initial NS5A screen results (Pichlmair et al., 2012), the original samples were re-analyzed on a hybrid linear trap quadrupole (LTQ) Orbitrap Velos. We identified a total of 274 proteins, compared to the 50 detected in the first analysis. A caveat of improved sensitivity is the higher detection rate of non-specific binding proteins. In order to filter false-positive interactors more efficiently, we included additional negative controls available from the recently published CRAPome repository (www.crapome.org) in our analysis. All identified protein interactions were scored using spectral counts to calculate both the SAINT probability and fold change (FC_B) score (Choi et al., 2011; Mellacheruvu et al., 2013). A SAINT probability ≥ 0.9 and an FC_B score ≥ 4 was used as threshold to enrich for high confidence interactors, leaving a total of 24 proteins (Fig. 1A), 50% of which overlapped with our previously published data set (supplemental table 1). In addition, 15 from the 24 were either already validated as NS5A-binding partners or have been confirmed in a study published during the preparation of this manuscript by Germain et al., using a similar experimental approach (supplemental table 1) (Germain et al., 2014).

In addition to the previously characterized NS5A-binding proteins Ubiquitin Specific Peptidase 19 (USP19) and Amphiphysin II (BIN1), one of the highest ranking proteins was the KMT SMYD3 (Masumi et al., 2005; Pichlmair et al., 2012; Zech et al., 2003). This finding is consistent with two previous studies, that further corroborated our results (de Chassey et al., 2008; Germain et al., 2014). Since none of these studies had confirmed the SMYD3–NS5A interaction, we verified it by employing Myc-tagged NS5A and HA-tagged SMYD3 that were co-expressed in HEK 293T cells and subjected to co-immunoprecipitation (co-IP) assays. As shown in Fig. 1B, SMYD3 co-purified with immunoprecipitated NS5A and vice versa when the reciprocal co-IP was performed. The catalytic activity of SMYD3 was not relevant for the association, since NS5A interacted just as strongly with a point mutant of SMYD3 (Y239F) previously described to be catalytically inactive (Foreman et al., 2011; Xu et al., 2011). Finally, we confirmed the interaction of endogenous SMYD3 with TAP-tagged NS5A expressed in doxycyline-regulated HEK Flp-In cells (Fig. 1D) (Pichlmair et al., 2012).

To further characterize the interaction, we aimed to map the region in SMYD3 bound by NS5A. SMYD3 is a two-lobed protein: the N-terminal region harbors the catalytic SET-domain, which is split by a MYND-domain, a zinc-finger motif mediating protein–protein and protein–DNA interactions (Hamamoto et al., 2004). The C-terminal lobe consists of three tetratricopeptide repeat motifs and is proposed to have a regulatory role in SMYD3 activity by blocking the substrate binding site. Based on the crystal structure of SMYD3, internal deletion mutants were cloned. These lacked surface exposed areas or regions lining the catalytic site (Fig. 2A) (Foreman et al., 2011; Sirinupong et al., 2010; Xu et al., 2011). Although none of the mutants resulted in a complete loss of NS5A-binding, the deletion of the MYND-domain (mutant SΔ2) severely impaired the interaction. The mutant SΔ3 lacking the adjacent residues 88–124 also exhibited reduced binding to NS5A, suggesting that the MYND-domain is either improperly folded in this mutant, or that the binding region extends into the SET-domain (Figs. 2B and C). In addition SMYD3 SΔ2 failed to co-localize with Myc-NS5A when co-transfected in Hela cells (Supplemental Fig. 1).

Next, we investigated which region of NS5A interacted with SMYD3. Of note, attempts to co-precipitate SMYD3 with immunopurified NS5A using a monoclonal mouse anti-NS5A antibody (9E10) failed, suggesting antibody binding may overlap with the SMYD3 binding site (data not shown). Since the antibody detects an epitope in DIII, we generated NS5A mutants lacking parts of the C-terminal portion of the protein (Fig. 2D). As shown in Fig. 2E and F, deleting residues encompassing DII had no effect on the interaction with SMYD3, whereas the absence of residues

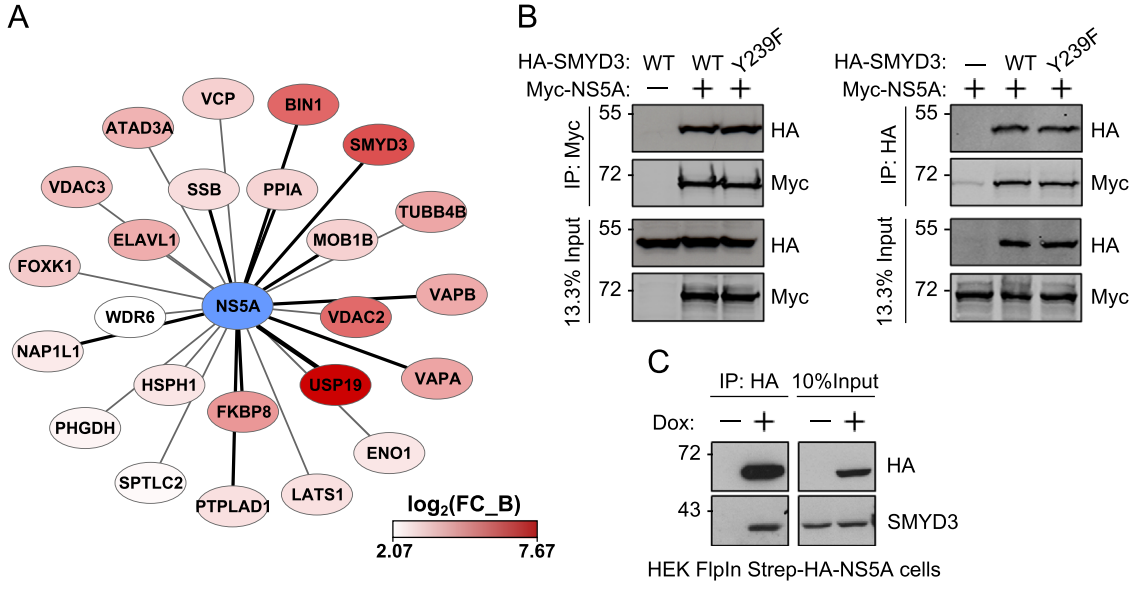

Fig. 1. Identification and confirmation of SMYD3 as interactor of NS5A. (A) Schematic representation of NS5A-binding proteins identified by TAP-MS with an FC_B score ≥ 4. Node color gradient corresponds to increasing $\log_2$ FC_B scores. Known interactions are depicted by black edges, novel interactions by gray edges. NS5A is highlighted in blue. Two biological replicates were analyzed as technical duplicates. (B) Interaction of overexpressed SMYD3 and NS5A. Myc-NS5A, HA-SMYD3 or catalytic inactive SMYD3 (Y239F) were transiently expressed in HEK 293T cells. 48 h posttransfection, protein complexes were immunoprecipitated and analyzed by Western blot. Representative blots of 3 independent experiments are shown. (C) Interaction of endogenous SMYD3 with TAP-tagged NS5A. Expression of NS5A in HEK FlpIn Strep-HA-NS5A cells was induced by addition of 1 μg/ml doxycyline. After 48 h, NS5A was immunoprecipitated and samples analyzed by Western blot.

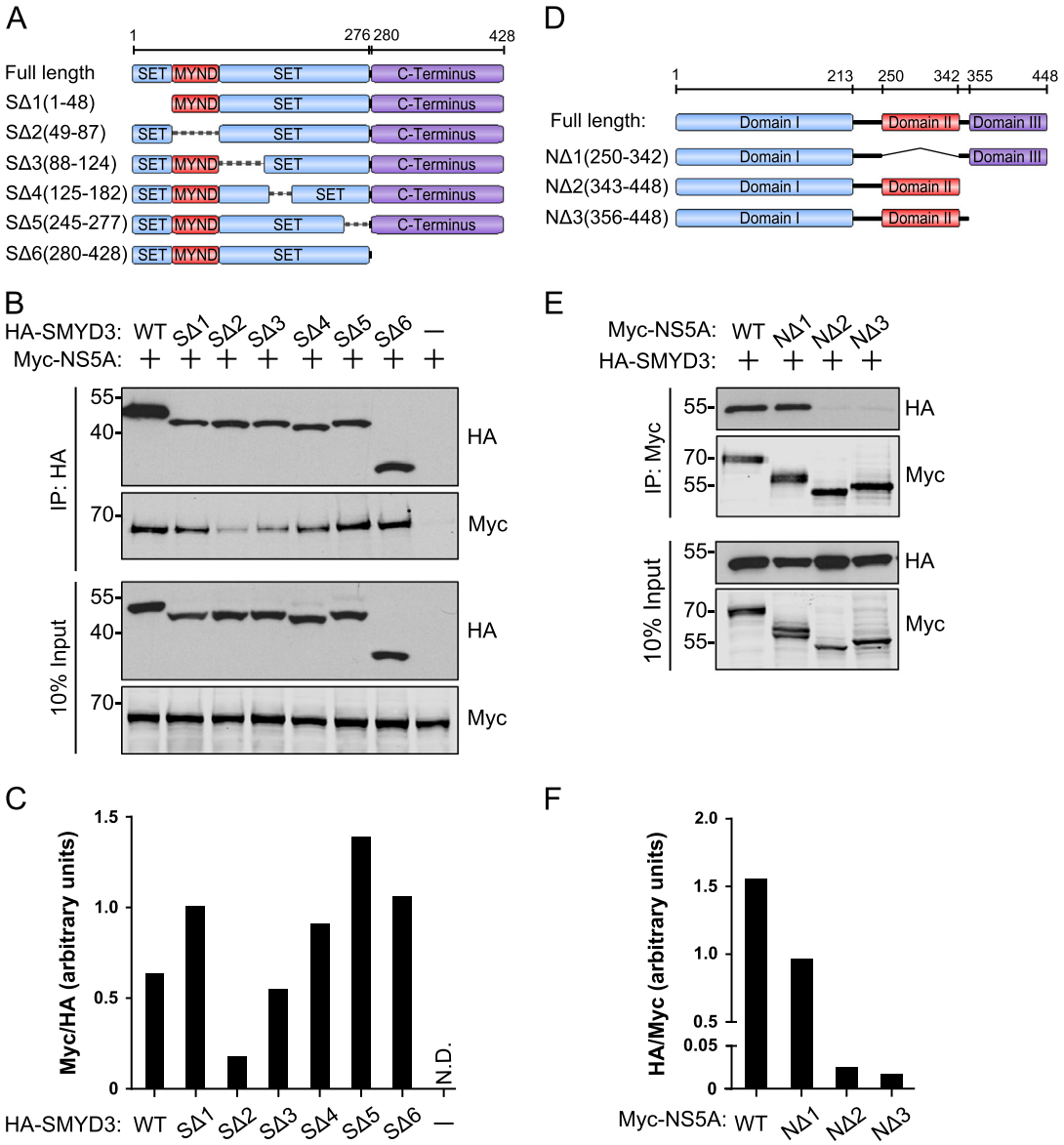

Fig. 2. Mapping the binding sites of SMYD3 and NS5A. (A) Schematic representation of full-length SMYD3 and respective deletion mutants. The N-terminal lobe contains the catalytic SET-domain (blue), which is split by the zinc-finger MYND-domain (red). The second lobe consists of regulatory C-terminal domain (purple). Residues spanning the individual domains are indicated. (B) Association of Myc-tagged NS5A with HA-tagged SMYD3 deletion mutants. The indicated plasmids were co-expressed in HEK 293T cells and co-immunoprecipitation experiments were performed as in Fig. 1B. (C) Ratio of co-purified NS5A with the respective SMYD3 mutants. Bars represent the ratio of quantified band signals of the Western blots shown above. (D) Schematic representation of full-length NS5A and respective deletion mutants. NS5A consists of 3 domains (blue, red and purple, respectively) connected by two low-complexity sequences (black). Residues spanning the individual domains are indicated. (E) Association of HA-tagged SMYD3 with Myc-tagged NS5A deletion mutants. The indicated plasmids were co-expressed in HEK 293T cells and co-immunoprecipitation experiments were performed as in (B). (F) Ratio of co-purified SMYD3 with the respective NS5A mutants. Bars represent the ratio of quantified band signals of the Western blots shown above. (B and E) Representative blots of at least 2 similar experiments are shown.

343–448, which correspond to LCSII and DIII, abolished SMYD3 binding. The LCSII contains numerous prolines, a common recognition motif of MYND-domains (Ansieau and Leutz, 2002). To distinguish if either LCSII or DIII were responsible for the interaction, we included an additional mutant lacking only DIII. The presence, however, of the polyproline motif in LCSII did not restore SMYD3 binding, meaning that the association is mediated by DIII. Taken together, our results confirm SMYD3 as specific binding partner of NS5A and identify the SMYD3 MYND-domain and DIII of NS5A as regions mediating the interaction.

To validate these results in a more authentic system we evaluated if SMYD3 also interacted with NS5A in the context of an active viral replicase. To this end, we generated Huh7.5 cells stably expressing HA-tagged SMYD3 (Huh7.5/HA-SMYD3). Previous reports have shown that adding an N-terminal tag to SMYD3 does not interfere with its catalytic activity, nor does it seem to alter its subcellular localization (Fig. 3E) (Foreman et al., 2011; Hamamoto et al., 2004; Kunizaki et al., 2007). Huh7.5/HA-SMYD3 cells were then electroporated with RNA encoding the genotype 2a subgenomic JFH1 replicon, or the full-length genome of the chimeric strain termed Jc1, which produces high amounts of infectious particles in culture (Pietschmann et al., 2006). In both cases, NS5A co-precipitated with HA-SMYD3 (Fig. 3A and C). NS5A exists in a basal and a hyperphosphorylated state. Based on apparent molecular weight, these are commonly referred to as p56 and p58, respectively (Tanji et al., 1995). Interestingly, we found the p58 form preferentially co-precipitated with SMYD3 (Fig. 3B and D).

In addition, we used immunofluorescence to examine the localization of SMYD3 with subgenomic replicon-derived NS5A

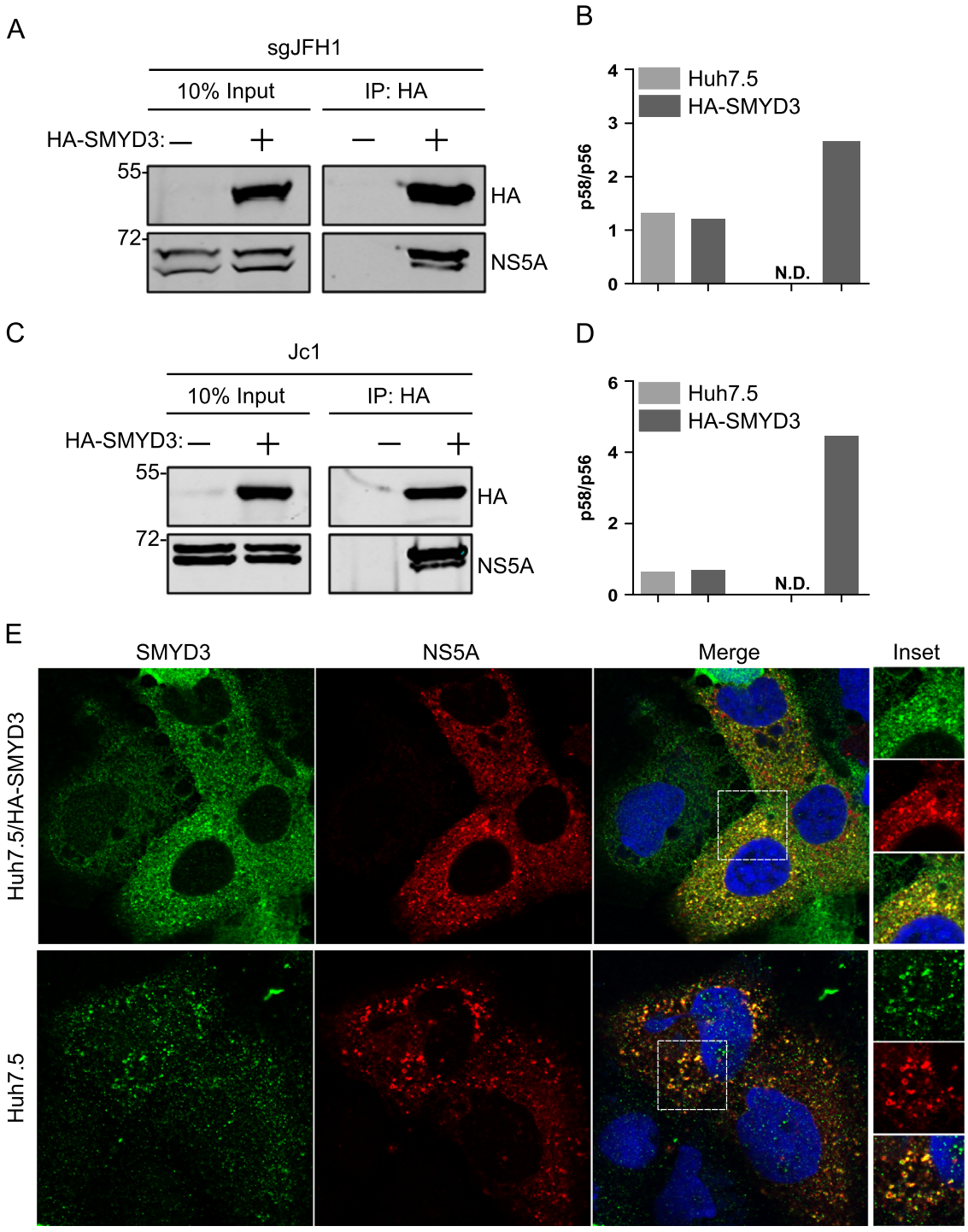

Fig. 3. Interaction of SMYD3 with NS5A in the context of viral replication. (A and C) Huh7.5/HA-SMYD3 cells were electroporated with RNA encoding the JFH1 subgenomic replicon (sgJFH1) or full-length Jc1. 72 h post electroporation, HA-SMYD3 was immunoprecipiated and analyzed by Western blot using anti-HA and anti-NS5A antibodies. (B and D) Enrichment of hyperphosphorylated NS5A (p58) in SMYD3 pull-downs. Western blot bands shown in (A) and (C) corresponding to the p56 and p58 phosphoforms of NS5A were quantified and the p58/P56 ratio calculated. (E) Co-localization of overexpressed HA-SMYD3 (top panel) or endogenous SMYD3 with subgenomic JFH1 NS5A. Huh7.5 cells were electroporated as described above. After 48 h, cells were fixed and proteins stained using SMYD3 (green) and NS5A (red) antibodies. Nuclei were counterstained with DAPI. Images were analyzed by confocal microscopy. Co-localization was quantified using ImageJ and the WCIF 'Intensity Correlation Analysis' plugin (upper panel: R_r=0.746; R=0.903; lower panel: R_r=0.620; R=0.781).

in Huh7.5 cells. In accordance with previous studies, NS5A localized to cytoplasmic, most often perinuclear foci (Fig. 3E insets) (Gosert et al., 2003). In some instances, NS5A staining appeared as ring-like structures, probably corresponding to lipid droplets decorated with this protein (Appel et al., 2008). As shown in Fig. 3E, NS5A clearly co-localized with HA-tagged overexpressed as well as endogenous SMYD3. The latter is of particular importance, as attempts to detect an interaction between NS5A and endogenous SMYD3 were not successful, due to the lack of a suitable anti-SMYD3 antibody to immunoprecipitate the endogenous protein (data not shown). Collectively, our data reveal that SMYD3 and NS5A also interact and co-localize with each other in the context

of active viral replication. Furthermore, the fact that SMYD3 associates also with genotype 2a NS5A indicates that the interaction is not genotype-specific.

SMYD3 is upregulated in various types of cancer, in particular colon, breast, prostate and liver carcinomas, where it exhibits potent growth promoting effects. Interestingly, RNAi-mediated knockdown of SMYD3 has been shown to result in cell cycle arrest and apoptosis of different cancer cell lines, including the human hepatoma cell line Huh7, from which Huh7.5 and Huh7-Lunet cells used in this study are derived (Blight et al., 2002; Chen et al., 2007; Friebe et al., 2005; Hamamoto et al., 2004; Ren et al., 2010). In order to investigate if SMYD3 had a role in the HCV life cycle, but at the same time avoid off-target effects due to RNAi-induced cytotoxicity associated with SMYD3 knockdown, we generated a Huh7-Lunet-derived cell pool stably overexpressing wildtype SMYD3 (Lunet/S3) or the catalytically inactive point mutant SMYD3 Y239F (Lunet/YF) (Fig. 4A) that was still capable of interacting with NS5A (Fig. 1B).

First, we analyzed whether SMYD3 had an effect on viral RNA replication kinetics. To this end, stable Huh7-Lunet/S3 or Lunet/YF cells were electroporated with subgenomic JFH-1 reporter replicon RNA and viral replication was quantified by measuring Firefly luciferase activity in cell lysates harvested at several time points after transfection. As shown in Fig. 4B, luciferase activities were similar for each cell line, excluding a role of SMYD3 in viral replication. Similar results were obtained for the full-length, infectious *Renilla luciferase* reporter virus JcR2A (Fig. 4C) (Reiss et al., 2011). Next, we assessed if SMYD3 influenced infectious virion production in the form of infectious particles release relative to viral replication (Infectivity/replication). For this purpose we infected naïve Huh7.5 cells with supernatants harvested from JcR2a-transfected Lunet/S3, Lunet/YF or Lunet/GFP cells and quantified Renilla activity 48 h post infection. Interestingly, relative infectivity of virus particles released from Lunet/S3 cells was more than 3-fold lower as compared to GFP-control cells. This effect appeared to be specific as it was not observed in cells overexpressing catalytic inactive SMYD3 (Fig. 4D). To distinguish if this defect occurred at the level of virus particle assembly or release, we determined relative infectivity in cell culture supernatants and corresponding cell lysates that were prepared by repeated cycles of freezing and thawing (extra- and intracellular infectivity, respectively). Naive Huh7.5 cells were inoculated with the respective fractions and luciferase activity was determined 48 h later. As shown in Fig. 4E, cells overexpressing wildtype SMYD3 exhibited a reduction of relative intra- as well as extracellular infectivity amounts (5-fold and 2-fold, respectively), whereas titers of Lunet/YF cells were similar to Lunet-GFP cells, arguing that SMYD3 impaired infectious particle assembly.

To corroborate this observation, we repeated this experiment by using a reporter-free virus genome and more direct assays. The

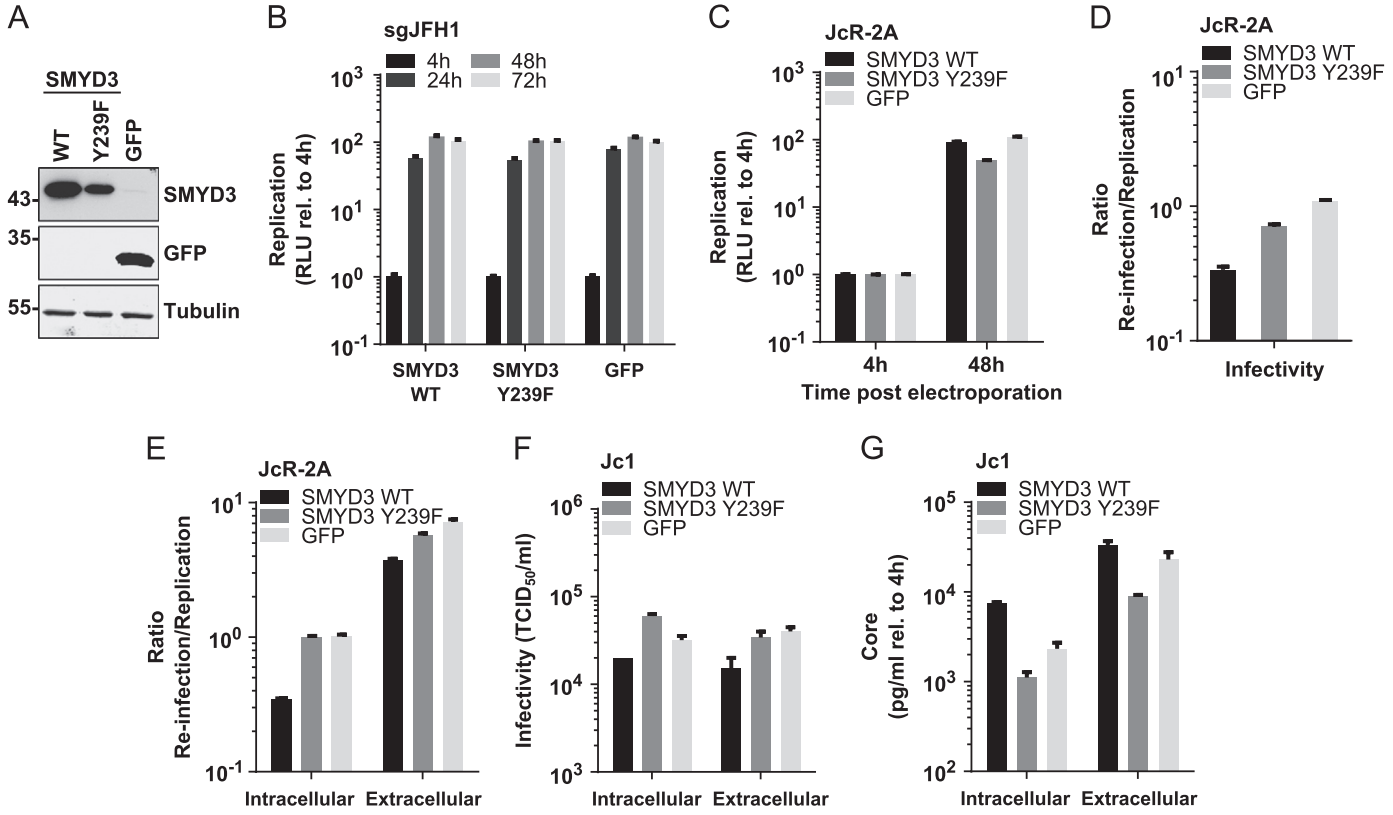

Fig. 4. SMYD3 is a negative regulator of HCV infectious particle assembly. (A) Western blot analysis of Huh7-Lunet cells stably expressing wildtype (WT) SMYD3, catalytic inactive (Y239F) SMYD3 or GFP. (B) Effect of SMYD3 overexpression on HCV RNA replication kinetics. Indicated cell lines were electroporated with RNA encoding the subgenomic JFH1 luciferase reporter replicon. Viral replication was measured at the indicated time points by luciferase assay. Luciferase activity is expressed in relative light units (RLU) normalized to the 4 h value to account for different transfection efficiencies. (C) Effect of SMYD3 overexpression on replication of the full-length infectious Renilla reporter virus JcR-2A. Indicated cell lines were electroporated with JcR-2A RNA and harvested after 4 and 48 h. Viral replication was quantified as mentioned above. (D) Effect of SMYD3 overexpression on JcR-2A relative infectivity. Supernatants from (C) were harvested at the indicated time points and used to inoculate naïve Huh7.5 cells in duplicate. 48 h post infection, Renilla activity in reinfected cells was measured as in (B) Viral infectivity is expressed as ratio of re-infection over replication. (E) JcR-2A intra- and extracellular infectivity. Cells pellets and supernatants of cells transfected with JcR-2A RNA were subjected to 3 freeze-thaw cycles 48 h postelectroporation. Viral infectivity in the respective fractions was determined as mentioned above. (F) Effect of SMYD3 overexpression on intra- and extracellular virus titers of the non-reporter virus Jc1. The different Huh7-Lunet cell lines were transfected with Jc1 RNA. 48 h postelectroporation, cell pellets and supernatants were treated by freezing and thawing as described above. Viral infectivity was determined by limiting dilution assay and data are represented as $TCID_{50}$/ml. (G) Intra- and extracellular amounts of HCV core protein. Core levels in cell lysates and corresponding supernatants were determined by core-specific ELISA 4 and 48 h postelectroporation of Jc1 RNA. Concentrations of core are depicted as pg/ml normalized to intracellular core levels 4 h post electroporation to account for different transfection efficiencies. Bars represent mean values and standard error of the means from 3 (JcR-2A) or 2 (sgJFH1 and Jc1) independent experiments.

individual cell lines were electroporated with RNA encoding the chimeric virus Jc1 and after 48 h intra- and extracellular virus titers were quantified by limiting dilution assay ($TCID_{50}$/ml) (Fig. 4F) In addition, we determined concentrations of HCV core protein in cell lysates and supernatants by core ELISA (Fig. 4F).In accordance with our previous results, virus titers were 4 times lower in Lunet/S3 cells, whereas overexpressing catalytically inactive SMYD3 resulted in titers similar to GFP control cells (Fig. 4F). Interestingly, the reduction in virus titers coincided with an overall intracellular accumulation of core protein (Fig. 4G), with levels detected in Lunet/S3 cells on average three times higher compared to GFP control cells.

To exclude the possibility that SMYD3 overexpression influenced the cellular secretory capacity in general, we transfected the different Huh7-Lunet cell lines with a plasmid encoding the naturally secreted *Gaussia luciferase* (G-luc) and monitored G-luc activity in the supernatants over time. Protein secretion was almost identical among the different cell lines, indicating that the reduction of virus titers in response to SMYD3 overexpression was specific for HCV assembly and not the consequence of impaired protein secretion (supplemental Fig. 2). Taken together, our data suggest that SMYD3 negatively regulates virus particle production by interfering with the assembly process of infectious virions, which is reflected in form of reduced virus titers and an overall accumulation of intracellular core protein.

As mentioned in the introduction, NS5A is a multitasking protein, coordinating various stages of the viral life cycle, as well as interfering with many different host cellular pathways. It is believed, that different NS5A interactions with viral and cellular proteins, presumably regulated by the NS5A phosphorylation state, determine its functional state (Cordek et al., 2011; Huang et al., 2007). As shown here and in earlier studies, one of these interaction partners is SMYD3. To date, very little is known about its physiological role. Given that lysine methylation is increasingly recognized as an important post-translational modification regulating protein function and fine-tuning many essential signaling pathways, one might speculate that SMYD3 is a component of one or more cellular processes that are involved in virus production (Erce et al., 2012). Alternatively, SMYD3 might be involved in the modification and impairment of other HCV proteins required for assembly. Binding to SMYD3 would therefore allow NS5A to counteract SMYD3 function and ensure productive virion assembly. This hypothesis is supported by the fact that NS5A interacted with SMYD3 through DIII, the domain essential for virus formation (Appel et al., 2008, 2005; Hughes et al., 2009; Tellinghuisen et al., 2008a).

Conclusion

In summary, we report the identification of the lysine methyl transferase SMYD3 as a binding partner of HCV NS5A. Using cell lines overexpressing wildtype or non-functional SMYD3, we identified SMYD3 as potential negative regulator of HCV infectious particle assembly. Further studies, in particular regarding the cellular function and targets of SMYD3, may aid to gain more mechanistic insight into SMYD3-mediated assembly inhibition and help to decipher the still only partially understood HCV assembly process.

Materials and methods

Liquid chromatography mass spectrometry and data validation

TAP-MS analyses of NS5A-associated protein complexes has been performed as previously described (Pichlmair et al., 2012). The same samples were re-analyzed by liquid chromatography mass spectrometry (LCMS) on a hybrid linear trap quadrupole (LTQ) Orbitrap Velos (ThermoFisher Scientific) coupled to an Agilent 1200 series HPLC (Agilent technologies) as previously described (Huber et al., 2014). The list of all identified proteins was uploaded to the 'Contaminant Repository for Affinity Purification-Mass spectrometry data (CRAPome) repository' (www.crapome.org) and filtered against a set of 17 negative control samples. Negative control samples were chosen according to the following criteria: cell line (HEK 293), epitope tag (Strep-HA), subcellular fraction (total cell lysate), instrument type (LTQ Orbitrap Velos). Spectral count data was used to calculate the 'Significance Analysis of Interactome' (SAINT) probability (low mode = 0, min fold = 1, Normalize = 1) and a fold change score (FC_B; default settings) (Choi et al., 2011; Mellacheruvu et al., 2013). Both scoring tools are available on the repository website. Proteins were first filtered based on a SAINT probability ≥ 0.9, followed by a second filter corresponding to a FC_B score ≥ 4. The NS5A interactome was visualized using cytoscape (www.cytoscape.org).

Cell lines and cell culture

All cell lines were maintained in Dulbecco's Modified Eagle Medium (Gibco) supplemented with 10% FCS (Invitrogen), 2 mM Glutamine and antibiotics (100 U/ml penicillin and 100 mg/ml streptomycin). HEK FlpIn Strep-HA-NS5A cells have been described previously (Pichlmair et al., 2012).The human hepatoma cell line Huh7.5 was purchased from *Apath* LLC (St. Louis, MO). Huh7-Lunet cells have been described previously (Friebe et al., 2005; Koutsoudakis et al., 2006). Cells stably expressing SMYD3, SMYD3 Y239F, GFP or HA-SMYD3 were generated by lentiviral transduction and selected and maintained in DMEM containing 5 μg/ml of puromycin.

Plasmid constructs

Expression vectors encoding full-length or truncated proteins were generated by Gateway® recombination reactions (Invitrogen) as described previously (Pichlmair et al., 2012). Expression vectors used in this study were: pcDNA-N-2HA-TEV-GW and pCS2-N-6xMyc-GW for transient expression in HEK 293T cells and pWPI-GW and pWPI-N-HA-GW for the generation of lentiviral particles. Internal and point mutations were introduced by site-directed mutagenesis (Agilent Technologies) of the respective pDONR201 vectors according to the manufacturer's instructions. All primer sequences used in this study are available upon request.

Plasmids pFK_i389LucNS3-3′JFH_δg (sgJFH1), pFK-J6/Core-846/JFH1_wt_δg (Jc1) and pFK_i389-JcR2a_δg_JC1 (JcR2a) encoding the JFH1 subgenomic reporter replicon, the full-length chimeric genome Jc1 and the Jc-1 derived reporter virus JcR-2A, respectively, have been described recently (Kaul et al., 2007; Pietschmann et al., 2006; Reiss et al., 2011).

Lentiviral gene transduction

Huh7-Lunet and Huh7.5 cells stably expressing SMYD3, SMYD3 Y239F, GFP or HA-SMYD3, respectively, were generated by lentiviral transduction. For lentivirus production, HEK 293T were seeded in 6-well plates and co-transfected with the respective lentiviral vector pWPI (1 μg), the packaging vector pCMVR8.91 (750 ng) and the envelope vector pMD.G (250 ng) using Lipofectamine2000 (Invitrogen) as recommended by the manufacturer. Target cells were seeded in a 6-well plate and infected with filtered viral supernatants harvested after 48 h. Transduced cells were selected by addition of 5 μg/ml puromycin 24 h post infection. SMYD3 WT, SMYD3 Y239F or GFP expression was analyzed by Western blot using rabbit anti-SMYD3 (Abcam, 1:2000) or mouse anti-GFP (Roche, 1:5000) antibodies.

Co-Immunoprecipiations

HEK 293T cells were co-transfected with the indicated plasmids using Polyfect (QIAGEN) according to the manufacturer's protocol. The amount of DNA per plasmid was adjusted to achieve equal expression. Total levels of transfected DNA were kept constant by the addition of empty vector. For co-precipitation of endogenous SMYD3 with TAP-tagged NS5A: HEK FlpIn cells inducibly expressing NS5A fused to a tandem Strep-tag II-hemagglutinin (Strep-HA or TAP-tag) were cultured in the presence of 1 μg/ml doxycline. 48 h post transfection or doxycycline induction, cells were lysed in IP-buffer (50 mM Tris/HCl pH 8.0, 150 mM NaCl, 1%NP40, 5 mM EDTA, 5 mM EGTA, protease inhibitor cocktail (Roche), 50 mM NaF and 1 mM Na_3VO_4) and cleared by centrifugation. 1.5 or 2 mg of total protein was incubated with anti-HA, or anti-Myc agarose beads (SIGMA) for 1.5 h at 4 °C. Beads were washed 3 × with IP-buffer and then eluted in 5% (v/v) SDS/PBS. Immunoprecipitates were analyzed by Western blot using the tag-specific directly conjugated antibodies rabbit anti-Myc IRDye™800 (Rockland) and mouse anti HA7-HRP (SIGMA) as indicated. Endogenous SMYD3 in HEK FlpIn cells was detected using rabbit anti-SMYD3 as mentioned above. NS5A expressed in the context of the subgenomic or full-length replicons was detected using the monoclonal mouse anti-NS5A 9E10 (1:10,000; kind gift from Prof. Charles Rice; Rockefeller University, New York). Bands were quantified using the ImageJ software (Schneider et al., 2012).

Confocal microscopy

Huh7.5 wildtype or Huh7.5/HA-SMYD3 cells electroporated with subgenomic JFH1 replicon transcripts were grown on coverslips for 72 h. Cells were rinsed with PBS, fixed with 4% paraformaldehyde for 15 min, and then permeabilized with 0.1% Triton X-100 for 15 min. After rinsing with PBS, cells were blocked with 5% goat serum (GS) for 1 h. Cells were stained with rabbit anti-SMYD3 (1:300; Abcam) and mouse anti-NS5A (1:1000; 9E10) diluted in 5% GS for 1 h. After four washes with PBS, slips were incubated in the dark with Alexa Fluor 488 anti-rabbit and 568 anti-mouse secondary antibodies (both 1:1000 in 5%GS; Molecular Probes) for 1 h. Nuclei were counterstained with DAPI. Cover slips were mounted on glass slides using ProLong Gold Antifade reagent (Invitrogen). Images were acquired using a Zeiss LSM 700 confocal laser scanning microscope. Co-localization of fluorescence signals was evaluated quantitatively for Pearson's correlation coefficient (R_r) and Manders coefficient (R) by using the 'Image J' software and the 'Intensity Correlation Analysis' plugin.

RNA in vitro transcription and electroporation

in vitro transcription of *Mlu*I-linearized plasmids was performed as described previously (Krieger et al., 2001). Briefly, 5–10 μg of linearized plasmids were in vitro transcribed in an overnight reaction using T7 RNA polymerase and terminated by the addition of DNAse. RNA was extracted with acidic phenol and chloroform, precipitated in isopropanol and the pellet dissolved in H_2O. RNA integrity was assessed by agarose gel electrophoresis.

For electroporation of in vitro transcribed RNA, 1×10^7 cells/ml of Huh7-Lunet cells were suspended in cytomix supplemented with 2 mM ATP, pH 7.6 and 5 mM glutathione (van den Hoff et al., 1990). 200 μl of cell suspension were mixed with 5 μg of RNA, transferred to an electroporation cuvette (gap width of 0.2 cm) and electroporated using the BioRad Gene Pulser System at 975 μF and 166 V. Cells were immediately transferred to 13 ml of fresh medium and seeded as described below. For co-precipitation experiments, 1.5×10^7 cells/ml of Huh7.5 or Huh7.5/HA-SMYD3 cells were suspended in cytomix as above. 400 μl of cell suspension was mixed with 7.5 μg of RNA and electroporated in cuvettes with a 0.4 gap width at 975 μF and 270 V. Cells were then resuspended in 20 ml DMEM, transferred to 15 cm^2 dishes and incubated for 72 h.

Replication and infectivity assays

Quantification of Firefly or Renilla luciferase activity as readout for sgJFH1 and JcR2A replication, respectively, was performed as described previously (Reiss et al., 2011). Briefly, cells were lysed in 300 μl (6-well plate) of lysis buffer at the indicated time points post electroporation. Luminescence in 20 μl of lysate was quantified in technical duplicates for 10 s in a luminometer (Lumat LB9507; Berthold, Freiburg, Germany). Relative light units (RLUs) were normalized to the respective 4 h value to account for differences in transfection efficiency.

To measure JcR-2A infectivity, supernatants were collected 48 h post electroporation and used to inoculate naïve Huh7.5 cells seeded in 24-well plates the day before (5×10^4 ml^{-1}). Renilla activity was measured 48 h post reinfection as described above. Jc1 infectivity was determined by limiting dilution assay on Huh7.5 cells (Lindenbach et al., 2005). Positive cells were stained with a mouse monoclonal NS3 (2E3) antibody and HRP-conjugated anti-mouse polyclonal antibody (Sigma) (Backes et al., 2010). To measure intra- and extracellular infectivity, electroporated (Jc1 or JcR-2A) cells were seeded on 10 cm^2 dishes. After 48 h, cells were harvested and subjected to multiple freeze-thaw cycles as described previously (Gastaminza et al., 2006). Viral titers of the respective fractions were determined as described above.

Core ELISA

To quantify HCV core protein amounts, transfected cells were seeded into 6-well plates (2 ml/well). After 48 h, cell culture supernatants were filtered through 45 μm filters and diluted 1:2 with PBS supplemented with 1% Triton X-100. To determine intracellular core amounts, cell monolayers were washed twice with PBS and lysed by addition of 0.5 ml PBS containing 0.5% Triton X-100 and 1 mM PMSF, 0.1 μg/ml Aprotinin and 4 μg/ml Leupeptin. Lysates were cleared by centrifugation at 10,000 RPM for 10 min at 4 °C. HCV core protein was quantified in the Central Laboratory of the University Hospital Heidelberg (Analysezentrum, Heidelberg, Germany). If required, samples were diluted with PBS containing 0.5% Triton X-100.

Acknowledgments

The work of C.A.E was supported by the Austrian Science Fund (FWF W1205-B09, CCHD PhD program). Work of R.B. is supported by the Deutsche Forschungsgemeinschaft (Transregional Collaborative Research Project TR83, TP13 and Collaborative Research Project 638, TP A5). We thank Prof. Charles M. Rice for the kind gift of the monoclonal mouse anti-NS5A antibody (Rockefeller University, New York); Roberto Giambruno, Marielle Klein, Berend Snijder and Richard Kumaran Kandasamy for critical comments on the manuscript.

Appendix A. Supporting information

Supplementary data associated with this article can be found in the online version at http://dx.doi.org/10.1016/j.virol.2014.05.016.

References

Ansieau, S., Leutz, A., 2002. The conserved Mynd domain of BS69 binds cellular and oncoviral proteins through a common PXLXP motif. J. Biol. Chem. 277, 4906–4910.

Appel, N., Pietschmann, T., Bartenschlager, R., 2005. Mutational analysis of hepatitis C virus nonstructural protein 5A: potential role of differential phosphorylation in RNA replication and identification of a genetically flexible domain. J. Virol. 79, 3187–3194.

Appel, N., Zayas, M., Miller, S., Krijnse-Locker, J., Schaller, T., Friebe, P., Kallis, S., Engel, U., Bartenschlager, R., 2008. Essential role of domain III of nonstructural protein 5A for hepatitis C virus infectious particle assembly. PLoS Pathog. 4, e1000035.

Backes, P., Quinkert, D., Reiss, S., Binder, M., Zayas, M., Rescher, U., Gerke, V., Bartenschlager, R., Lohmann, V., 2010. Role of annexin A2 in the production of infectious hepatitis C virus particles. J. Virol. 84, 5775–5789.

Bartenschlager, R., Penin, F., Lohmann, V., André, P., 2011. Assembly of infectious hepatitis C virus particles. Trends Microbiol. 19, 95–103.

Blight, K.J., McKeating, J.A., Rice, C.M., 2002. Highly permissive cell lines for subgenomic and genomic hepatitis C virus RNA replication. J. Virol. 76, 13001–13014.

Brass, V., Bieck, E., Montserret, R., Wolk, B., Hellings, J.A., Blum, H.E., Penin, F., Moradpour, D., 2002. An amino-terminal amphipathic alpha-helix mediates membrane association of the hepatitis C virus nonstructural protein 5A. J. Biol. Chem. 277, 8130–8139.

Chen, L.-B., Xu, J.-Y., Yang, Z., Wang, G.-B., 2007. Silencing SMYD3 in hepatoma demethylates RIZI promoter induces apoptosis and inhibits cell proliferation and migration. World J. Gastroenterol. 13, 5718–5724.

Choi, H., Larsen, B., Lin, Z.-Y., Breitkreutz, A., Mellacheruvu, D., Fermin, D., Qin, Z.S., Tyers, M., Gingras, A.-C., Nesvizhskii, A.I., 2011. SAINT: probabilistic scoring of affinity purification-mass spectrometry data. Nat. Methods 8, 70–73.

Cock-Rada, A.M., Medjkane, S., Janski, N., Yousfi, N., Perichon, M., Chaussepied, M., Chluba, J., Langsley, G., Weitzman, J.B., 2012. SMYD3 promotes cancer invasion by epigenetic upregulation of the metalloproteinase MMP-9. Cancer Res. 72, 810–820.

Cordek, D.G., Bechtel, J.T., Maynard, A.T., Kazmierski, W.M., Cameron, C.E., 2011. Targeting the NS5A protein of HCV: an emerging option. Drugs Future 36, 691–711.

Davis, K.L., Mitra, D., Medjedovic, J., Beam, C., Rustgi, V., 2011. Direct economic burden of chronic hepatitis C virus in a United States managed care population. J. Clin. Gastroenterol. 45, e17–24.

de Chassey, B., Navratil, V., Tafforeau, L., Hiet, M.S., Aublin-Gex, A., Agaugué, S., Meiffren, G., Pradezynski, F., Faria, B.F., Chantier, T., Le Breton, M., Pellet, J., Davoust, N., Mangeot, P.E., Chaboud, A., Penin, F., Jacob, Y., Vidalain, P.O., Vidal, M., André, P., Rabourdin-Combe, C., Lotteau, V., 2008. Hepatitis C virus infection protein network. Mol. Syst. Biol., 4.

Erce, M.A., Pang, C.N.I., Hart-Smith, G., Wilkins, M.R., 2012. The methylproteome and the intracellular methylation network. Proteomics 12, 564–586.

Foreman, K.W., Brown, M., Park, F., Emtage, S., Harriss, J., Das, C., Zhu, L., Crew, A., Arnold, L., Shaaban, S., Tucker, P., 2011. Structural and functional profiling of the human histone methyltransferase SMYD3. PLoS ONE 6, e22290.

Friebe, P., Boudet, J., Simorre, J.P., 2005. Kissing-loop interaction in the 3′ end of the hepatitis C virus genome essential for RNA replication. J. Virol. 79, 380–392.

Gastaminza, P., Kapadia, S.B., Chisari, F.V., 2006. Differential biophysical properties of infectious intracellular and secreted hepatitis C virus particles. J. Virol. 80, 11074–11081.

Germain, M.A., Chatel-Chaix, L., Gagne, B., Bonneil, E., Thibault, P., Pradezynski, F., de Chassey, B., Meyniel-Shicklin, L., Lotteau, V., Baril, M., Lamarre, D., 2014. Elucidating novel hepatitis C virus/host interactions using combined mass spectrometry and functional genomics approaches. Mol. Cell. Proteomics 13, 184–203.

Gosert, R., Egger, D., Lohmann, V., Bartenschlager, R., Blum, H.E., Bienz, K., Moradpour, D., 2003. Identification of the hepatitis C virus RNA replication complex in Huh-7 cells harboring subgenomic replicons. J. Virol. 77, 5487–5492.

Hamamoto, R., Furukawa, Y., Morita, M., Iimura, Y., Silva, F.P., Li, M., Yagyu, R., Nakamura, Y., 2004. SMYD3 encodes a histone methyltransferase involved in the proliferation of cancer cells. Nat. Cell Biol. 6, 731–740.

Huang, Y., Staschke, K., De Francesco, R., Tan, S.-L., 2007. Phosphorylation of hepatitis C virus NS5A nonstructural protein: a new paradigm for phosphorylation-dependent viral RNA replication? Virology 364, 1–9.

Huber, M.L., Sacco, R., Parapatics, K., Skucha, A., Khamina, K., Müller, A.C., Rudashevskaya, E.L., Bennett, K.L., 2014. abFASP-MS: affinity-based filter-aided sample preparation mass spectrometry for quantitative analysis of chemically labeled protein complexes. J. Proteome Res. 13, 1147–1155.

Hughes, M., Griffin, S., Harris, M., 2009. Domain III of NS5A contributes to both RNA replication and assembly of hepatitis C virus particles. J. Gen. Virol. 90, 1329–1334.

Kaul, A., Woerz, I., Meuleman, P., Leroux-Roels, G., Bartenschlager, R., 2007. Cell culture adaptation of hepatitis C virus and in vivo viability of an adapted variant. J. Virol. 81, 13168–13179.

Koutsoudakis, G., Herrmann, E., Kallis, S., Bartenschlager, R., Pietschmann, T., 2006. The level of CD81 cell surface expression is a key determinant for productive entry of hepatitis C virus into host cells. J. Virol. 81, 588–598.

Krieger, N., Lohmann, V., Bartenschlager, R., 2001. Enhancement of hepatitis C virus RNA replication by cell culture-adaptive mutations. J. Virol. 75, 4614–4624.

Kunizaki, M., Hamamoto, R., Silva, F.P., Yamaguchi, K., Nagayasu, T., Shibuya, M., Nakamura, Y., Furukawa, Y., 2007. The lysine 831 of vascular endothelial growth factor receptor 1 is a novel target of methylation by SMYD3. Cancer Res. 67, 10759–10765.

Lindenbach, B.D., Evans, M.J., Syder, A.J., Wolk, B., 2005. Complete replication of hepatitis C virus in cell culture. Science 280, 747–749.

Masaki, T., Suzuki, R., Murakami, K., Aizaki, H., Ishii, K., Murayama, A., Date, T., Matsuura, Y., Miyamura, T., Wakita, T., Suzuki, T., 2008. Interaction of hepatitis C virus nonstructural protein 5A with core protein is critical for the production of infectious virus particles. J. Virol. 82, 7964–7976.

Masumi, A., Aizaki, H., Suzuki, T., DuHadaway, J.B., Prendergast, G.C., Komuro, K., Fukazawa, H., 2005. Reduction of hepatitis C virus NS5A phosphorylation through its interaction with amphiphysin II. Biochem. Biophys. Res. Commun. 336, 572–578.

Mellacheruvu, D., Wright, Z., Couzens, A.L., Lambert, J.-P., St-Denis, N.A., Li, T., Miteva, Y.V., Hauri, S., Sardiu, M.E., Low, T.Y., Halim, V.A., Bagshaw, R.D., Hubner, N.C., al-Hakim, A., Bouchard, A., Faubert, D., Fermin, D., Dunham, W.H., Goudreault, M., Lin, Z.-Y., Badillo, B.G., Pawson, T., Durocher, D., Coulombe, B., Aebersold, R., Superti-Furga, G., Colinge, J., Heck, A.J.R., Choi, H., Gstaiger, M., Mohammed, S., Cristea, I.M., Bennett, K.L., Washburn, M.P., Raught, B., Ewing, R. M., Gingras, A.-C., Nesvizhskii, A.I., 2013. The CRAPOME: A contaminant repository for affinity purification mass spectrometry data. Nat. Methods 10, 730–736.

Mohd Hanafiah, K., Groeger, J., Flaxman, A.D., Wiersma, S.T., 2013. Global epidemiology of hepatitis C virus infection: new estimates of age-specific antibody to HCV seroprevalence. Hepatology 57, 1333–1342.

Penin, F., Brass, V., Appel, N., Ramboarina, S., Montserret, R., Ficheux, D., Blum, H.E., Bartenschlager, R., Moradpour, D., 2004. Structure and function of the membrane anchor domain of hepatitis C virus nonstructural protein 5A. J. Biol Chem. 279, 40835–40843.

Pichlmair, A., Kandasamy, K., Alvisi, G., Mulhern, O., Sacco, R., Habjan, M., Binder, M., Stefanovic, A., Eberle, C.-A., Goncalves, A., Bürckstümmer, T., Müller, A.C., Fauster, A., Holze, C., Lindsten, K., Goodbourn, S., Kochs, G., Weber, F., Bartenschlager, R., Bowie, A.G., Bennett, K.L., Colinge, J., Superti-Furga, G., 2012. Inhibitome. Nature 487, 486–490.

Pietschmann, T., Kaul, A., Koutsoudakis, G., Shavinskaya, A., Kallis, S., Steinmann, E., Abid, K., Negro, F., Dreux, M., Cosset, F.-L., Bartenschlager, R., 2006. Construction and characterization of infectious intragenotypic and intergenotypic hepatitis C virus chimeras. Proc. Natl. Acad. Sci. U.S.A 103, 7408–7413.

Reiss, S., Rebhan, I., Backes, P., Romero-Brey, I., Erfle, H., Matula, P., Kaderali, L., Poenisch, M., Blankenburg, H., Hiet, M.-S., Longerich, T., Diehl, S., Ramirez, F., Balla, T., Rohr, K., Kaul, A., Bühler, S., Pepperkok, R., Lengauer, T., Albrecht, M., Eils, R., Schirmacher, P., Lohmann, V., Bartenschlager, R., 2011. Recruitment and activation of a lipid kinase by hepatitis C Virus NS5A is essential for integrity of the membranous replication compartment. Cell Host Microbe 9, 32–45.

Ren, T.-N., Wang, J.-S., He, Y.-M., Xu, C.-L., Wang, S.-Z., Xi, T., 2010. Effects of SMYD3 over-expression on cell cycle acceleration and cell proliferation in MDA-MB-231 human breast cancer cells. Med. Oncol.

Schneider, C.A., Rasband, W.S., Eliceiri, K.W., 2012. NIH Image to ImageJ: 25 years of image analysis. Nat. Methods 9, 671–675.

Sirinupong, N., Brunzelle, J., Doko, E., Yang, Z., 2010. Structural insights into the autoinhibition and posttranslational activation of histone methyltransferase SmyD3. J. Mol. Biol., 1–11.

Tanji, Y., Kaneko, T., Satoh, S., Shimotohno, K., 1995. Phosphorylation of hepatitis C virus-encoded nonstructural protein NS5A. J. Virol. 69, 3980–3986.

Tellinghuisen, T.L., Foss, K.L., Treadaway, J., 2008a. Regulation of hepatitis C virion production via phosphorylation of the NS5A protein. PLoS Pathog. 4, e1000032.

Tellinghuisen, T.L., Foss, K.L., Treadaway, J.C., Rice, C.M., 2008b. Identification of residues required for RNA replication in domains II and III of the hepatitis C virus NS5A protein. J. Virol. 82, 1073–1083.

Tellinghuisen, T.L., Marcotrigiano, J., Gorbalenya, A.E., Rice, C.M., 2004. The NS5A protein of hepatitis C virus is a zinc metalloprotein. J. Biol. Chem. 279, 48576–48587.

van den Hoff, M.J., Labruyère, W.T., Moorman, A.F., Lamers, W.H., 1990. The osmolarity of the electroporation medium affects the transient expression of genes. Nucl. Acids Res. 18, 6464.

Xu, S., Wu, J., Sun, B., Zhong, C., Ding, J., 2011. Structural and biochemical studies of human lysine methyltransferase Smyd3 reveal the important functional roles of its post-SET and TPR domains and the regulation of its activity by DNA binding. Nucl. Acids Res. 39, 4438–4449.

Zech, B., Kurtenbach, A., Krieger, N., Strand, D., Blencke, S., Morbitzer, M., Salassidis, K., Cotten, M., Wissing, J., Obert, S., Bartenschlager, R., Herget, T., Daub, H., 2003. Identification and characterization of amphiphysin II as a novel cellular interaction partner of the hepatitis C virus NS5A protein. J. Gen. Virol. 84, 555–560.